R. & M. No. 3391

MINISTRY OF AVIATION

AERONAUTICAL RESEARCH COUNCIL
REPORTS AND MEMORANDA

On the Shear Flexibility of Twisted Panels

By S. KELSEY and D. F. PILKINGTON

(Imperial College of Science and Technology)

On the Shear Flexibility of Twisted Panels

By S. Kelsey and D. F. Pilkington

(Imperial College of Science and Technology)

Summary.

A simple theoretical analysis is given for the additional shear flexibility of a twisted panel caused by bending of the panel under a shear loading. Results of some experiments on initially twisted sandwich panels show good agreement with the theory.

1. *Introduction.*

1.1. For the analysis of stressed skin structures, it is customarily assumed that the skin carries only a membrane type of stress distribution. In particular, the skin panels are often regarded as fulfilling a shear-carrying role, direct stresses being concentrated into effective booms in the idealised structure. The loading on such a shear panel is defined by the shear flow in it and its flexibility arises solely from the shear strains associated with the membrane shear-stress system in the panel. Single curvature of the panel, and also taper lead to no difficulties, since in both cases the concept of a membrane stress system remains valid and a suitable average stress flow or resultant can be defined to allow adequately for the effects of taper.

If, however, the panel surface exhibits twist relative to the axes Oxy for which the shear flow q is defined, then the membrane stress system gives rise to a resultant loading per unit area

$$p_q = 2q\partial^2 w_0/\partial x \, \partial y \tag{1.1}$$

normal to the local surface where $w_0 (x, y)$ measures the initial displacement of the panel surface from the xy plane (Fig. 1). In the absence of an equilibrating pressure, it is clear that the shear flow cannot exist alone in the twisted panel and must be accompanied by bending. Because of the bending, the stiffness of the panel as a shear-resistant structural element is reduced. The twisted panel as an element in a stressed skin structure and the specification of a statically equivalent force system acting on it is discussed in Section 9 of Ref. 2. It is the purpose of the present paper to investigate the reduction in shear stiffness for the simple case of a rectangular panel, supported on all edges and with a constant rate of twist $\phi = \partial^2 w_0/\partial x \, \partial y$. A simple theoretical analysis is developed and experimental results in good agreement with theory are reported.

1.2. It is first necessary to define the shear loading on a twisted panel. For the panel with all edges supported, the simplest loading of this type consists of a shear flow q acting in the mean projected plane of the panel. To analyse the stresses in the plate, we may resolve the loading into a membrane system, together with its equilibrating pressure, and a plate bending system, associated with the negative of this pressure. Provided the twist of the surface is small, its effect on the

---

bending deflections of the panel under pressure can be ignored, the analysis of which may therefore be based on a flat rectangular plate. However, because of the twist, the bending deflections result in a further shear strain, i.e. additional to that caused by the membrane shear stress. In Section 2, it is shown that the total shear strain in the plane of the loading is

$$\gamma_{xy} = q/Gt + 4\phi^2 q\bar{\omega} \tag{1.2}$$

where $\bar{\omega}$ is the average deflection of the panel under a unit normal pressure.

1.3. The main part of the theoretical analysis therefore consists of the determination of the average deflection parameter $\bar{\omega}$ for rectangular plates. This is straightforward by the classical plate theory and results are tabulated and shown graphically for the two cases of all edges simply supported and all edges clamped. For the clamped edges the method given by Timoshenko in Ref. 1 was used.

Since, however, the tests reported here were carried out on panels of sandwich construction, it was necessary to allow also for the effect of transverse shear flexibility on the plate normal deflections. Although a general approach to this by way of the Reissner equations is possible, a different method was adopted in order to give convenient correction terms to the results already obtained. An upper bound to the average deflection increment due to shear flexibility was calculated by means of the Principle of Virtual Forces[3] (Unit Load Method), assuming the shear-stress distribution given by the standard plate theory. To obtain a corresponding lower bound, the Principle of Virtual Displacements, in conjunction with a kinematic simplification of the shear-strain system, was used. These bounds coincide for a panel with simply supported edges and give a range of 3% total deflection for the test panels with clamped edges.

1.4. An experimental verification of the general result (Section 1.2), for the increase of shear flexibility, is reported in Section 4. Shear tests were carried out on panels with two different rates of twist (0·5 deg/in. and 1·0 deg/in.) in a square, four-hinged shear rig. Although in principle such a test rig is simple, the practical production of one which will consistently ensure a uniform shear field in the test specimen proves very difficult. Values of shear flexibility measured this way tend to be unreliable owing, *inter alia*, to the uncertainty of the specimen boundary conditions, its fit in the rig, the deformations of the rig itself, and the friction at its hinges. Thus, a direct comparison of shear stiffness between different specimens with differing rates of twist is not satisfactory for the measurement of comparatively small differences in their flexibility.

To overcome these difficulties, the range of tests on each specimen was extended to include the simultaneous application of a normal pressure p, proportional to the shear flow q, which also gives rise to shear deformation in the mean plane of the panel. The measurement of shear strain under this combined loading thus gave a wider confirmation of the theoretical analysis and largely eliminated the random and unpredictable differences between specimens.

Besides the overall panel shear strain, normal deflections and the bending strains were also measured. These results, shown in Section 4, also agree satisfactorily with the theoretical analysis.

2. *Shear of a Twisted Panel.*

Consider the twisted rectangular panel shown in Fig. 1. Its middle surface is defined by the equation

$$w_0 = \phi xy \tag{2.1}$$

where

$$\phi = \partial^2 w / \partial x\, \partial y \tag{2.2}$$

2

is the constant rate of twist of the surface relative to the axes shown. The panel is supported at the edges and is subjected to a loading defined by a constant shear flow q, acting in the twisted middle surface, together with a normal pressure p. Since the shear flow equilibrates a normal pressure,

$$p_a = -2\phi q \tag{2.3}$$

we can separate the stress systems in the panel into the two components shown in Fig. 2. The first of these (a) consists of the membrane shear system together with its equilibrating pressure p_a, while in the second (b) there is a total uniform pressure

$$p_b = p + 2\phi q \tag{2.4}$$

which must be carried by bending of the panel. The distribution of the transverse edge reactions in system (b) follows from analysis of the plate bending and depends on the proportions of the plate and on the support conditions along the panel edges.

In the case of zero applied pressure, p, bending arises only from the shear flow pressure, $2\phi q$. The related support reactions, together with the shear flow, q, then yield a boundary force pattern defining the shear-carrying function of the twisted panel as a structural element. For a square panel, the resultants on the four sides are easily seen to be statically equivalent to a shear flow q acting on the projected panel in the xy-plane. If the panel is rectangular, then the resultant on each edge does not lie in the xy-plane since the transverse component is, in general, no longer proportional to the length of the edge. Nevertheless, the panel loading may still be uniquely defined by the magnitude of the shear flow q, in this plane. This system does satisfy all conditions of equilibrium, so that any further boundary loads can only consist of a self-equilibrating set of transverse support reactions. Corresponding to this specification of the loading, the shear strain of the twisted panel, supported on all its edges is the projected shear strain in the xy-plane. Such a shear strain arises, not only through the membrane strains q/Gt, but also due to the bending of the panel. If the edge supports deflect under load, then the self-equilibrating support reactions will also do work and the physical interpretation of the generalised strain, corresponding to the load system specified by q, is not so simple. However, for the representation of the twisted panel as a structural element, it is sufficient to consider such additional work as arising from an increased flexibility of the system, under the shear flow q, and due to the support deflections. In the present paper, we restrict ourselves to the case when the edge supports are rigid, so that the flexibility increase comes from the bending of the panel alone.

To estimate the shear strain of the twisted panel, we apply the Principle of Virtual Forces[3] and consider the general case when the panel is subject to a pressure load p as well as the shear flow q.

By definition, the virtual complementary work due to the virtual force system δq is

$$\delta W^* = ab\gamma\delta q. \tag{2.5}$$

The associated virtual complementary energy from the membrane system (a) is

$$(\delta U_i^*)_a = abq\delta q/Gt \tag{2.6}$$

while that of the bending stress system (b) is conveniently expressed in the form

$$(\delta U_i^*)_b = \iint w(x, y)\delta p_b \, dx \, dy. \tag{2.7}$$

3

In equation (2.7) $w(x, y)$ is the deflection of the panel under the pressure load p_b and δp_b is the virtual pressure resulting from δq. Equating $\delta U_i{}^*$ and δW, and substituting for δp_b, we find

$$\gamma = \frac{q}{Gt} + \frac{2\phi}{ab} \int \int w(x, y) dx\, dy. \qquad (2.8)$$

The same result may also be obtained by direct kinematic consideration. Following Ref. 1, we may easily show that the shear strain in the twisted surface, due to displacements u, v, w, is

$$\frac{q}{Gt} = \frac{\partial u}{\partial y} + \frac{\partial v}{\partial x} + \frac{\partial w_0}{\partial x} \frac{\partial w}{\partial y} + \frac{\partial w_0}{\partial y} \frac{\partial w}{\partial x}. \qquad (2.9)$$

The first two terms on the right-hand side of equation (2.9) give the shear strain in the xy-plane. Hence, substituting for w_0 and integrating over the panel, we find for the average shear strain

$$\gamma = \frac{q}{Gt} - \frac{\phi}{ab} \int \int \left\{ y \frac{\partial w}{\partial x} + x \frac{\partial w}{\partial y} \right\} dx\, dy. \qquad (2.10)$$

Upon integration by parts, and with $w = 0$ at the boundary, the integral in equation (2.10) reduces to the same form as in equation (2.8).

Provided the deflections w are small, they will be proportional to p_b and hence may be expressed as

$$w = p_b \omega \qquad (2.11)$$

where $\omega(x, y)$ is the deflection function for the panel under unit pressure. If also the initial twist ϕ is small, it can be ignored in the determination of ω, which becomes then the deflection function for a flat rectangular panel under unit pressure. Hence, using equations (2.11), (2.4) in (2.8), we finally obtain

$$\gamma = q/Gt + 2\phi(p + 2\phi q)\bar{\omega} \qquad (2.12)$$

where

$$\bar{\omega} = \frac{1}{ab} \int \int \omega(x, y) dx\, dy \qquad (2.13)$$

is the average deflection of the rectangular (flat) panel under a unit uniform pressure. The shear flexibility f_q of the twisted panel, relating overall shear strain to shear flow, is from equation (2.12):

$$f_q = f_0 + f_\phi \qquad (2.14)$$

where

$$f_0 = 1/Gt, \qquad f_\phi = 4\phi^2 \bar{\omega}. \qquad (2.15)$$

Equation (2.12) also indicates a cross-flexibility between pressure p and shear q on the twisted panel, which is consistent with the more obvious reciprocal relation

$$\bar{w} = (p + 2\phi q)\bar{\omega}. \qquad (2.16)$$

In the tests described in Section 4, a pressure loading p was applied proportional to q. For this case the influence of the pressure may be represented as an apparent change in the rate of twist ϕ. Thus, if we introduce the proportionality factor c, such that

$$p = 2\phi c q, \qquad (2.17)$$

the shear strain of the twisted panel under the combined loading will be the same as for one with a rate of twist ϕ_e under q alone, where

$$\phi_e = \phi \sqrt{(1 + c)}. \qquad (2.18)$$

4

3. *Deflections of Rectangular Panel.*

(a) *Standard Plate Theory.*

The analysis of the previous chapter shows that the overall shear strain of the twisted panel, due to its bending, depends only on the average normal deflection, $\bar{\omega}$, under a uniform, unit pressure. With all four edges of the plate simply supported, standard plate theory[1] gives for the deflection function of the plate

$$\omega(x, y) = \frac{4a^4}{\pi^5 D} \sum_{m \text{ odd}} \frac{(-1)^{(m-1)/2}}{m^5} Y_m \cos \frac{m\pi x}{a} \tag{3.1}$$

where

$$Y_m = 1 - \frac{\alpha_m \operatorname{th} \alpha_m + 2}{2 \operatorname{ch} \alpha_m} \operatorname{ch} \frac{m\pi y}{b} + \frac{1}{2 \operatorname{ch} \alpha_m} \frac{m\pi y}{b} \operatorname{sh} \frac{m\pi y}{b} \tag{3.2}$$

$\alpha_m = m\pi b/2a$ and D is the plate flexural stiffness, $\operatorname{th}(\ ) = \tanh(\ )$, $\operatorname{ch}(\ ) = \cosh(\ )$, etc. From equations (3.1) and (3.2)

$$\left(\frac{\bar{\omega} D}{a^4}\right) = \frac{4}{\pi^6} \sum_{m \text{ odd}} \frac{1}{m^6} \left\{ 3 - \frac{3 \operatorname{th} \alpha_m}{\alpha_m} - \operatorname{th}^2 \alpha_m \right\} \tag{3.3}$$

which is shown plotted against the ratio a/b in Fig. 3.

For the case of all edges of the plate built-in, we may obtain a solution by superimposing on the pressure loading the following two sets of symmetrical bending-moment distributions along the edges of the plate (Ref. 1):

$$\left.\begin{array}{l} (M_y)_{y=\pm b/2} = \displaystyle\sum_{m \text{ odd}} (-1)^{(m-1)/2} E_m \cos \frac{m\pi x}{a} \\[3mm] (M_x)_{x=\pm a/2} = \displaystyle\sum_{m \text{ odd}} (-1)^{(m-1)/2} F_m \cos \frac{m\pi y}{b} \end{array}\right\} \tag{3.4}$$

Using the results given in Ref. 1, Section 4.4, for the corresponding deflected shapes, the average deflections $\bar{\omega}_1$, $\bar{\omega}_2$, due to these bending-moment distributions are:

$$\left.\begin{array}{l} \bar{\omega}_1 = -\dfrac{a^2}{\pi^3 D} \displaystyle\sum_{m \text{ odd}} \dfrac{E_m}{m^3} \left[1 - \dfrac{\operatorname{th} \alpha_m}{\alpha_m} - \operatorname{th}^2 \alpha_m \right] \\[5mm] \bar{\omega}_2 = -\dfrac{b^2}{\pi^3 D} \displaystyle\sum_{m \text{ odd}} \dfrac{F_m}{m^3} \left[1 - \dfrac{\operatorname{th} \beta_m}{\beta_m} - \operatorname{th}^2 \beta_m \right] \end{array}\right\} \tag{3.5}$$

where

$$\beta_m = m\pi a/2b.$$

The Fourier coefficients E_m, F_m, are determined from the conditions of zero slope normal to the plate edges. For the i'th Fourier component of the slope $\partial w/\partial y$ at the edge $y = \pm b/2$, the typical equation may be written

$$\frac{1}{i^4} \left[\frac{\alpha_i}{\operatorname{ch}^2 \alpha_i} - \operatorname{th} \alpha_i \right] + \frac{e_i}{i} \left[\frac{\alpha_i}{\operatorname{ch}^2 \alpha_i} + \operatorname{th} \alpha_i \right] + \frac{8ai}{\pi b} \sum_{m \text{ odd}} \frac{f_m}{m^3} \frac{1}{(a^2/b^2 + i^2/m^2)^2} = 0 \tag{3.6}$$

Similarly, the condition for the i component of $\partial w/\partial x$ at the edge $x = \pm a/2$, after a little manipulation, becomes

$$\frac{b^2}{i^4 a^2} \left[\frac{\beta_i}{\operatorname{ch}^2 \beta_i} - \operatorname{th} \beta_i \right] + \frac{f_i}{i} \left[\frac{\beta_i}{\operatorname{ch}^2 \beta_i} + \operatorname{th} \beta_i \right] + \frac{8bi}{\pi a} \sum_{m \text{ odd}} \frac{e_m}{m^3} \frac{1}{(b^2/a^2 + i^2/m^2)^2} = 0 \tag{3.7}$$

where

$$e_i = -\pi^3 E_i/4a^2, \qquad f_i = -\pi^3 F_i/4a^2 \tag{3.8}$$

5

The slight asymmetry between the two equations (3.6) and (3.7) results from the same factor, a^2, in the denominators of the expression chosen for e_i, f_i in equation (3.8).

Equation (3.5) indicates that, in order to calculate accurate estimates of the average deflection, it is only necessary to know the first few Fourier coefficients E_m, F_m. Moreover, the smallness of the coupling coefficients between the E's and F's in equations (3.6) and (3.7) suggest that these may be determined with sufficient precision by restricting the, strictly infinite, sets of equations to a finite number. Trial calculations, for $b/a = 5$, with up to twenty equations, showed that an average total deflection with an error less than $0 \cdot 1\%$ could be obtained with the first six equations of each set. Values of e_m, f_m, for $m = 1$ to 11, and $1 \leqslant b/a \leqslant 5$, which were computed in this way, are given in Table 1. Using these and equations (3.3), (3.5), the total average deflection parameter for the plate with built-in edges was calculated and appears, plotted against the ratio, a/b, in Fig. 3. The limiting case, $a/b = 0$, is, of course, elementary, giving

$$(\bar{\omega} D / a^4)_{a/b=0} = 1/720 . \tag{3.9}$$

During the tests on twisted panels under shear and pressure loads, measurements were made of the central transverse deflections for comparison with theory. From the above, the central deflection under uniform, unit-pressure of a rectangular panel with simply supported edges is, according to classical plate theory:

$$\frac{\omega_c D}{a^4} = \frac{5}{384} - \frac{4}{\pi^5} \sum_{m \, \mathrm{odd}} \frac{(-1)^{(m-1)/2}}{m^5} \frac{\alpha_m \, \mathrm{th} \, \alpha_m + 2}{2 \, \mathrm{ch} \, \alpha_m} . \tag{3.10}$$

The additional central deflections caused by the edge moment distributions of equation (3.4), required to represent built-in boundary conditions, are

$$\left. \begin{aligned} \frac{\omega_{1c} D}{a^4} &= -\frac{2}{\pi^5} \sum_{m \, \mathrm{odd}} (-1)^{(m-1)/2} e_m \frac{\alpha_m \, \mathrm{th} \, \alpha_m}{m^2 \, \mathrm{ch} \, \alpha_m} \\ \frac{\omega_{2c} D}{a^4} &= -\frac{2}{\pi^5} \sum_{m \, \mathrm{odd}} (-1)^{(m-1)/2} f_m \frac{\beta_m \, \mathrm{th} \, \beta_m}{m^2 \, \mathrm{ch} \, \beta_m} \end{aligned} \right\} \tag{3.11}$$

(b) *Influence of Transverse Shear Strain.*

Although adequate for the estimation of the small deflections of a thin solid plate under lateral pressure, the classical plate theory employed in 3(a) ignores the effect of transverse shear strains and is therefore not sufficiently accurate for sandwich panels, the shear flexibility of whose cores may be quite large. The effect is particularly marked when the panel edges are built-in since (as shown in Fig. 3) the deflections due to the in-plane strains alone are considerably reduced by the action of the edge moments.

Strictly, the inclusion of transverse shear flexibility requires a reformulation of the plate equations and a more detailed specification of the boundary conditions[5]. It is, however, fairly straightforward to calculate upper and lower bounds for the effect of shear strains as a correction to the standard results. In the present problem, this approach provides limits which, although rather wide as a fraction of the shear correction itself, are sufficiently close in comparison with the total deflections.

Lower Limit.—If w_s is the additional deflection due to transverse shear, we assume that the relevant shear strains arise only from the slopes $\partial w_s/\partial x$, $\partial w_s/\partial y$, i.e. we write

$$\frac{\partial w_s}{\partial x} = \frac{\alpha S_x}{G_t h}, \qquad \frac{\partial w_s}{\partial y} = \frac{\alpha S_y}{G_t h} \tag{3.12}$$

6

where[1] S_x, S_y are the transverse shear forces per unit length, G_t is the transverse shear modulus, h the total panel thickness, and α a factor which takes account of the shear-stress distribution across the plate thickness. For a solid plate, $\alpha = 6/5$ and for a sandwich, $\alpha = 1$. A symmetrical displacement function for w_s, satisfying the condition of zero w_s at the boundary is:

$$w_s = \sum_{m\,\text{odd}} \sum_{n\,\text{odd}} pa_{mn} \cos\frac{m\pi x}{a} \cos\frac{n\pi y}{b} = p\omega_s. \tag{3.13}$$

Application of the Principle of Virtual Displacements determines the coefficients a_{mn} for a unit pressure:

$$a_{mn} = \frac{16\alpha}{\pi^4 G_t h} \frac{(-1)^{(m+n-2)/2}}{mn(m^2/a^2 + n^2/b^2)}. \tag{3.14}$$

From this result, the average deflection parameter due to transverse shear strain is

$$\frac{\bar{\omega}_s G_t h}{\alpha a^2} = \frac{64}{\pi^6} \sum_{m\,\text{odd}} \sum_{n\,\text{odd}} \frac{1}{m^2 n^2 (m^2 + n^2 a^2/b^2)} \tag{3.15}$$

which is shown graphically in Fig. 4.

At the centre of the panel

$$\frac{\omega_{sc} G_t h}{\alpha a^2} = \frac{16}{\pi^4} \sum_{m\,\text{odd}} \sum_{n\,\text{odd}} \frac{(-1)^{(m+n-2)/2}}{mn(m^2 + n^2 a^2/b^2)} \tag{3.16}$$

which, for a square plate, reduces to

$$\left(\frac{\omega_{sc} Gh}{\alpha a^2}\right)_{a=b} = 0\cdot 0736. \tag{3.17}$$

These results hold for both simply supported and built-in edges. Equation (3.15) is an underestimate in virtue of the limited mode of deformation permitted by the assumption of equation (3.12). Though the shear strains are inevitably compatible, the shear forces which they define are not necessarily in detailed equilibrium with the bending and twisting moments in the panel. Some qualification of the description 'simply supported edge' is also necessary, in that the above solution does not permit any shear strain in the plane of the edge. It is not therefore possible to make the twisting moments, M_{xy}, zero at the edges, which condition should also hold at a truly simply supported edge of a plate when transverse shear flexibility is admitted. The limited simple support which applies here gives only zero bending moment at the edges. For this case, however, the above result is exact, as shown by its concurrence with the calculated upper bound.

Upper Limit to $\bar{\omega}_s$.—To bound the average total deflection from above, we assume that the distribution of shear forces S_x, S_y throughout the plate is given by the solution according to classical plate theory, and apply the Unit Load Method. All stresses are now in equilibrium, but the strains are not necessarily compatible.

If S_x, S_y, s_x, s_y are the shear forces due to a unit pressure over the plate and to the unit load system respectively, then the Unit Load Method gives directly

$$\bar{\omega}_s = \frac{\alpha}{G_t h} \int_{-a/2}^{a/2} \int_{-b/2}^{b/2} \{S_x s_x + S_y s_y\} dx\,dy. \tag{3.16}$$

7

The statements on upper and lower bounds as yielded by the two methods are, of course, only applicable to the average deflection results. Equations (3.16), (3.17) for the central deflection can therefore only be regarded as an approximation for the effect of shear strain, and not as a lower limit.

4. *Experimental Work.*

Measurements of overall shear strain and central deflection of square, twisted sandwich panels, under shear and normal pressure were made in the rig shown in Figs. 5 and 6. It consists of the usual square frame, made up from four massive edge members hinged together at the corners, in which a pair of panels was mounted back-to-back. Shear load was produced by a tension or compression across the frame, applied to a diagonally opposite pair of hinge pins. The back-to-back mounting of two panels, as well as eliminating out-of-plane loads and consequent distortion of the frame, allowed a normal pressure to be applied by sealing and evacuating the space between them.

In order to define precisely the edges of the panel experiencing shear strain, these were cast with Araldite into slots in four solid-steel edge pieces which in turn fit and are bolted into the main channel-section edge members. The hinge pins are positioned at the corners of the square formed by the panel edges so as to give compatibility of shear strain in the panel and frame.

Shear-strain measurements were based on the diagonal extension and compression of the frame. Simple extensometers, consisting of dial gauges reading to 10^{-4} in., with extended probes, were attached on both sides of the frame to the hinge pins (Fig. 6). Dial gauges were also used to measure normal deflections at the centre of the panels. These were mounted from the back of the main frame members. Strictly, both these measurements are susceptible to error from any rig deformations, but independent tests showed any such effect to be negligible. In particular, the diagonal strains agreed very well (within 1%) with those recorded by strain gauges and an extensometer mounted directly on a flat panel tested in shear. Such direct measurement of the overall shear strain was not, of course, possible with twisted panels.

All panels tested were of honeycomb sandwich construction with 30 S.W.G. ($0 \cdot 0125$ in.) faces of aluminium alloy, the thickness of the faces being limited by the strength of the Araldite edge attachment. The panels were Redux bonded, using the blanket and vacuum method, on a jig with the appropriate twist. To ensure an accurate fit in the test rig, this latter was used as an assembly jig, the edge pieces being bolted tightly in place and the Araldite joints cast one at a time (after degreasing and etching with phosphoric acid) while the frame was clamped accurately square. The absence of serious building-in stresses was indicated by the ease with which the hinge pins could be rotated or withdrawn.

As an initial check on the design of the rig and the methods of measurement employed, first tests were carried out on flat panels. The degree of uniformity of shear strain achieved may be assessed from the direct strain distributions along the diagonals, shown in Fig. 7. Each point plotted there is the average of 16 individual strain-gauge measurements, i.e. four gauges measured with tension and compression applied in turn along each frame diagonal. Individual results in each set differed from the average by no more than about $2\frac{1}{2}$%, which is hardly more than the errors likely in the strain-gauge readings. The distribution along the loaded diagonal shows a greater variation from uniformity than that along the unloaded diagonal, presumably owing to slight rig deformation near the loaded corners. Nevertheless, these results suggest that, for the most part, the shear stress in the panel should be within about ± 5% of the average value.

As already mentioned, the overall shear strain deduced from the diagonal extension and contraction of the frame agreed closely with the average strain-gauge result and also with other methods. Moreover, individual panels gave repeatable results within the same limits of accuracy. In spite of this however, the shear modulus values calculated for the flat panels were disappointingly inaccurate. Tensile tests on sandwich specimens, in which E and ν were determined, gave a shear modulus of $3 \cdot 86 \times 10^6$ lb/in^2, while the shear rig yielded values between $4 \cdot 0$ and $4 \cdot 35 \times 10^6$ lb/in^2. Thus, not only did the shear rig overestimate the shear modulus, but also showed considerable scatter between nominally identical panels.

Both these effects are, at least qualitatively, explicable by the action of friction on the hinge pins, principally the loaded ones, of the shear frame. Ideally, the hinges to which no external load is applied, i.e. those on the horizontal diagonal in Fig. 6, should be completely unloaded. However, the presence of friction on the loaded pins, even if a state of pure shear in the panel is assumed, requires a tension across the 'unloaded' pins in order to cause the slight rotation of the edge members associated with shear strain. This tension reduces the shear load carried by the panel and hence its shear strain. That some such force did arise was indicated by the 'unloaded' pins tightening up progressively as the rig was loaded.

These errors did not, however, affect the tests of twisted panels since the loading of these with different combinations of shear and pressure provided a range of tests on the same panel without the necessity of removing it from the rig. Fig. 8 shows the results of shear-flexibility measurements on two pairs of twisted panels, having actual rates of twist of $0 \cdot 5$ and $1 \cdot 0$ deg/in. respectively. The results, plotted against equivalent rate of twist ϕ_e {equation (2.18)}, on a background of the theoretical estimates from Sections 2 and 3, are given relative to the shear flexibility of an effectively flat panel in each case, i.e. one with a combination of q and p such that

$$p_b = p + 2\phi q = 0. \tag{4.1}$$

The elastic constants used in the calculation derive from tensile tests on sandwich specimens for the face properties: $E = 10 \cdot 28 \times 10^6$ lb/in^2, $G = 3 \cdot 86 \times 10^6$ lb/in^2, $\nu = 0 \cdot 330$. For the honeycomb core, a theoretical estimate of the shear modulus based on Ref. 4, was used, giving $G_t = 3 \cdot 99 \times 10^4$ lb/in^2.

Measured effective shear moduli are given in Table 2 and again show a consistent error between the two pairs of panels and also with the flat ones tested earlier.

As described earlier, the pressure load on the panels was produced by sealing the volume between the panels and exhausting it with a vacuum pump, the pressure reduction being measured with a simple manometer. In the loading, pressure increments were always applied before the corresponding shear increments in order to give a uniform effect of friction.

In Fig. 9 the shear-strain measurements of a twisted panel under pressure alone are shown together with the corresponding theoretical curves. This result is of interest in displaying the small displacements which must be measured in this type of shear test.

Two further sets of results give the central deflections of a number of panels under different combined loadings in Fig. 10 and Fig. 11 the bending-strain distributions along the diagonals of a twisted panel under shear. The theoretical deflections shown in Fig. 10 use equation (3.17) to give an approximate correction for the effects of transverse shear strain. They are plotted as central deflections for unit diagonal load on the rig against the twist parameter

$$\phi(1 + c) = \phi + p/2q.$$

10

5. Conclusions.

A simple theoretical analysis has been developed for the decrease in effective shear stiffness of a rectangular panel which arises from the bending of the panel when it has a twisted surface. The main parameter in determining the loss of stiffness is the average normal deflection of the panel under a unit, uniform pressure.

Though classical plate theory is adequate for the determination of the average deflection parameter in solid panels, the additional influence of transverse shear flexibility is important in sandwich panels with shear-flexible cores. Upper and lower bounds for this effect have been evaluated by energy methods.

The predictions of the theory have been substantiated by the results of shear tests carried out on initially twisted sandwich panels.

NOTATION

$Oxyz$	Cartesian axes, Oz along mean normal to panel
u, v, w	Displacements at panel middle surface along Ox, Oy, Oz
w_0	Initial displacement of middle surface
E, G, G_t	Young's modulus, shear modulus, transverse shear modulus (for sandwich panel)
ν	Poisson's ratio
D	Flexural stiffness of panel
h	Depth of panel
t	Membrane thickness of panel
a, b	Dimensions of rectangular panel
ϕ	Rate of twist of panel middle surface
$\omega(x, y)$	Deflection of flat panel under unit normal pressure
q	Shear flow
M_x, M_y, S_x, S_y	Bending moments and shear forces per unit length
E_i, F_i	Fourier coefficients for edge bending-moment distributions
p	Normal pressure

REFERENCES

No.	Author(s)	Title, etc.
1	S. Timoshenko	*Theory of plates and shells.* McGraw Hill. 1940.
2	J. H. Argyris and S. Kelsey	*Modern fuselage analysis and the elastic aircraft.* Butterworths. 1963.
3	J. H. Argyris	*Energy theorems and structural analysis.* Butterworths. 1960.
4	S. Kelsey, R. A. Gellatly and B. W. Clark.	The shear modulus of foil honeycomb cores. *Aircraft Engineering*, Vol. 30, p. 294. 1958.
5	E. Reissner	The effect of transverse shear deformation on the bending of elastic plates. *J. App. Mech.*, Vol. 12, p. A69. 1945.

TABLE 1

Edge Moment Coefficients

b/a	1·00	1·05	1·10	1·15	1·20	1·40	1·60
e_1	+0·372084	+0·380661	+0·387505	+0·392864	+0·396979	+0·405060	+0·406500
e_3	−0·037918	−0·040438	−0·042529	−0·044235	−0·045608	−0·048693	−0·049691
e_5	−0·017560	−0·018001	−0·018351	−0·018627	−0·018843	−0·019335	−0·019596
e_7	−0·008272	−0·008402	−0·008509	−0·008598	−0·008674	−0·008920	−0·009172
e_9	−0·004376	−0·004434	−0·004487	−0·004536	−0·004584	−0·004788	−0·005037
e_{11}	−0·002546	−0·002583	−0·002620	−0·002658	−0·002698	−0·002883	−0·003111
f_1	+0·372084	+0·399200	+0·425057	+0·449527	+0·472538	+0·550072	+0·607247
f_3	−0·037918	−0·038683	−0·038877	−0·038498	−0·037559	−0·028772	−0·013777
f_5	−0·017560	−0·018790	−0·019938	−0·020994	−0·021951	−0·024719	−0·025788
f_7	−0·008272	−0·008952	−0·009625	−0·010284	−0·010926	−0·013268	−0·015185
f_9	−0·004376	−0·004755	−0·005140	−0·005527	−0·005914	−0·007437	−0·008868
f_{11}	−0·002546	−0·002768	−0·002996	−0·003230	−0·003469	−0·004447	−0·005430

b/a	1·8	2·0	2·5	3·0	3·5	4·0	5·0
e_1	+0·406065	+0·405420	+0·404522	+0·403994	+0·403344	+0·402529	+0·400621
e_3	−0·049994	−0·050183	−0·051021	−0·052387	−0·054066	−0·055875	−0·059221
e_5	−0·019863	−0·020208	−0·021397	−0·022858	−0·024384	−0·025826	−0·028111
e_7	−0·009482	−0·009853	−0·010952	−0·012132	−0·013255	−0·014244	−0·015704
e_9	−0·005333	−0·005665	−0·006570	−0·007466	−0·008275	−0·008961	−0·009938
e_{11}	−0·003372	−0·003652	−0·004375	−0·005056	−0·005651	−0·006145	−0·006835
f_1	+0·649183	+0·680347	+0·729850	+0·757564	+0·774557	+0·785698	+0·798903
f_3	+0·004968	+0·025467	+0·076083	+0·118580	+0·151277	+0·175789	+0·208117
f_5	−0·025257	−0·023247	−0·012668	−0·003493	−0·021997	−0·040316	−0·071629
f_7	−0·016639	−0·017606	−0·017754	−0·014640	−0·008684	−0·000676	+0·018040
f_9	−0·010165	−0·011301	−0·013270	−0·013777	−0·012724	−0·010194	−0·001669
f_{11}	−0·006388	−0·007296	−0·009236	−0·010522	−0·011020	·−0·010676	−0·007568

$$e_m = -\frac{\pi^3}{4a^2}E_m, \qquad f_m = -\frac{\pi^3}{4a^2}F_m$$

TABLE 2

Effective Shear Moduli of Twisted Sandwich Panels

| Effective Rate of Twist ϕ_e (deg/in.) | Effective Shear Modulus $G \times 10^{-6}$ (lb/in²) | | | |
| | Theory | | Experiment | |
	Max.	Min.	0·5°/in panel	1°/in panel
0	3·86	3·86	3·71	4·00
0·354	3·78	3·78	3·61	—
0·500	3·70	3·69	3·55	3·81
0·500	3·70	3·69	3·55†	—
0·613	3·63	3·62	3·48†	—
0·707	3·56	3·54	3·38†	3·64
0·790	3·49	3·47	3·28†	—
0·866	3·42	3·40	—	3·49
1·000	3·29	3·26	—	3·38
1·000	3·29	3·26	—	3·48†
1·118	3·18	3·15	—	3·38†
1·225	3·07	3·03	—	3·22†
1·323	2·97	2·93	—	3·09†
1·414	2·87	2·83	—	2·98†
1·581	2·70	2·65	—	2·78†
1·732	2·55	2·50	—	2·57†

† Direction of loading reversed in these tests.

14
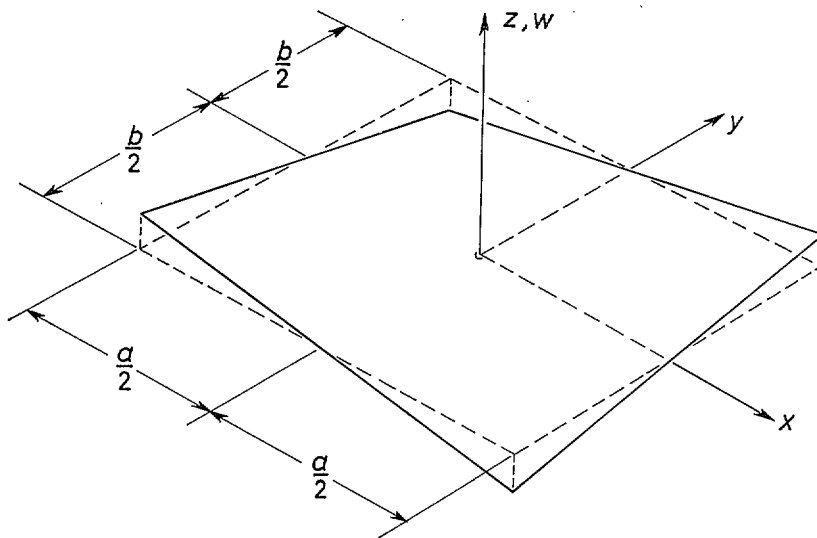
FIG. 1. Geometry of twisted panel.
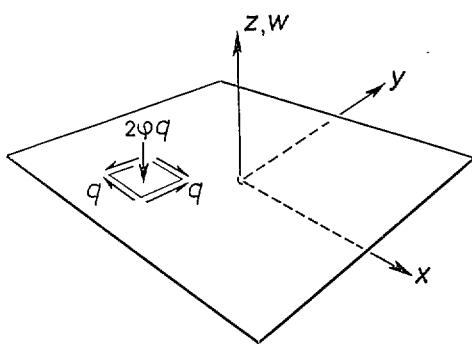
(a) Membrane Shear Flow.
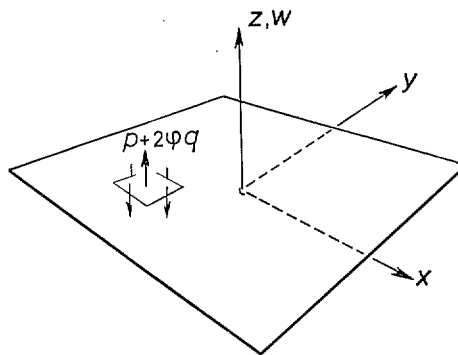
(b) Bending Stress System.

FIG. 2. Stress systems in twisted panel.

15

$\frac{\overline{\omega} D}{a^4} \times 10^{-3}$

$\frac{\overline{\omega} D}{a^4} \times 10^{-3}$

Simply Supported Edges.

Built in Edges.

a/b
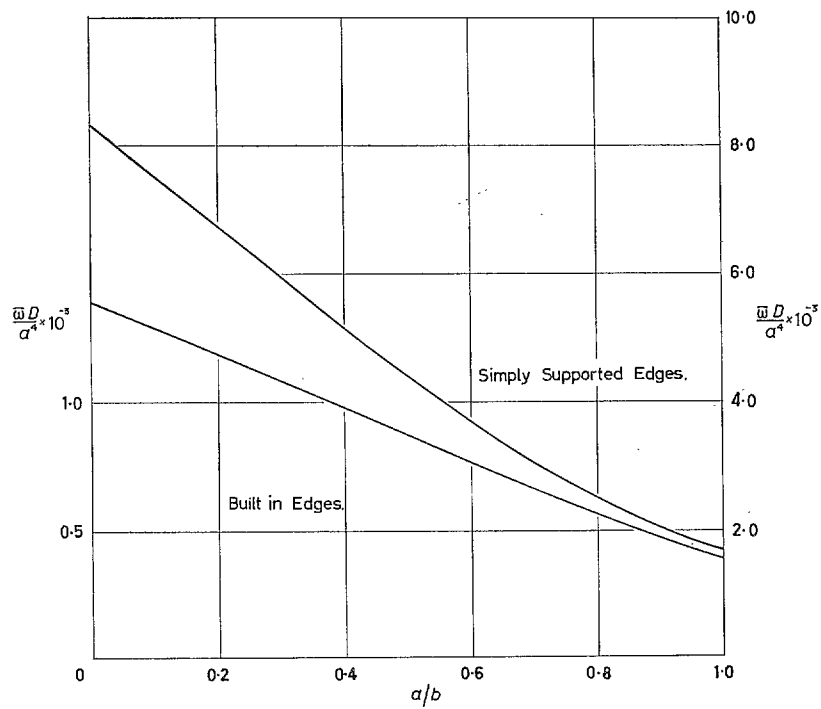
FIG. 3.   Average deflection of rectangular plate.

$\frac{\overline{\omega} G_s h}{a \, a^2}$

Upper Bound for Built in Edges.

Upper and Lower Bounds for Simply Supported Edges.

Lower Bound for Built in Edges.

a/b
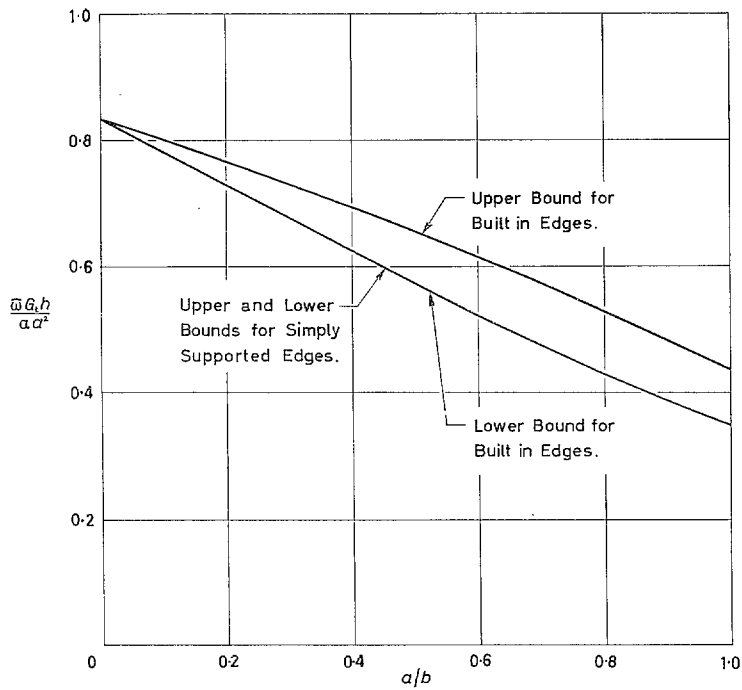
FIG. 4.   Average deflection of rectangular panel due to transverse shear strain.

16

Twisted Panel

Section XX

Hinge Pin

7″

10″

X

X

Loading Yoke
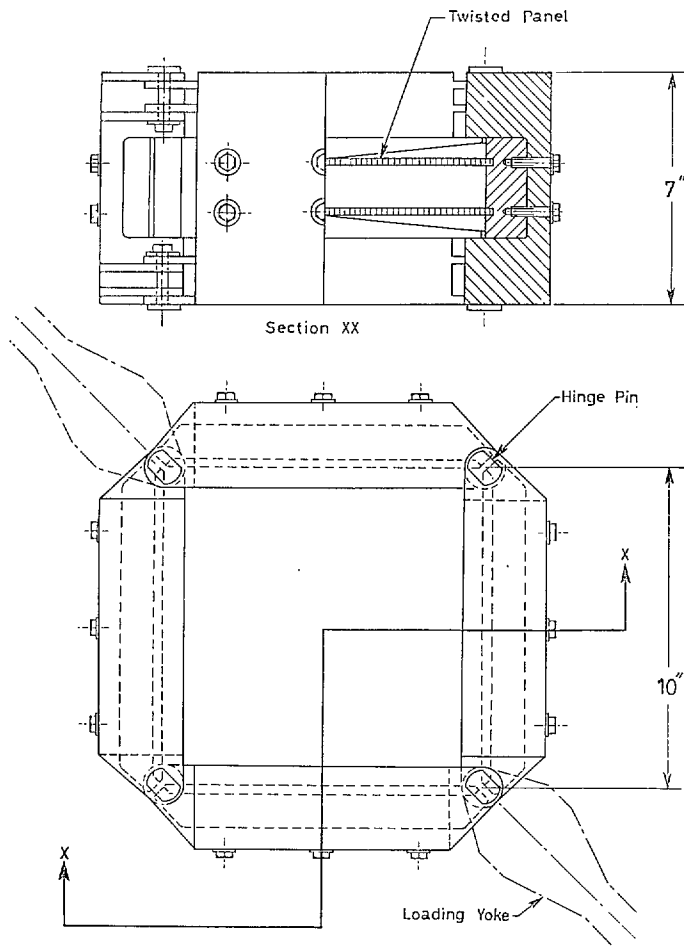
Fig. 5.   Test rig.
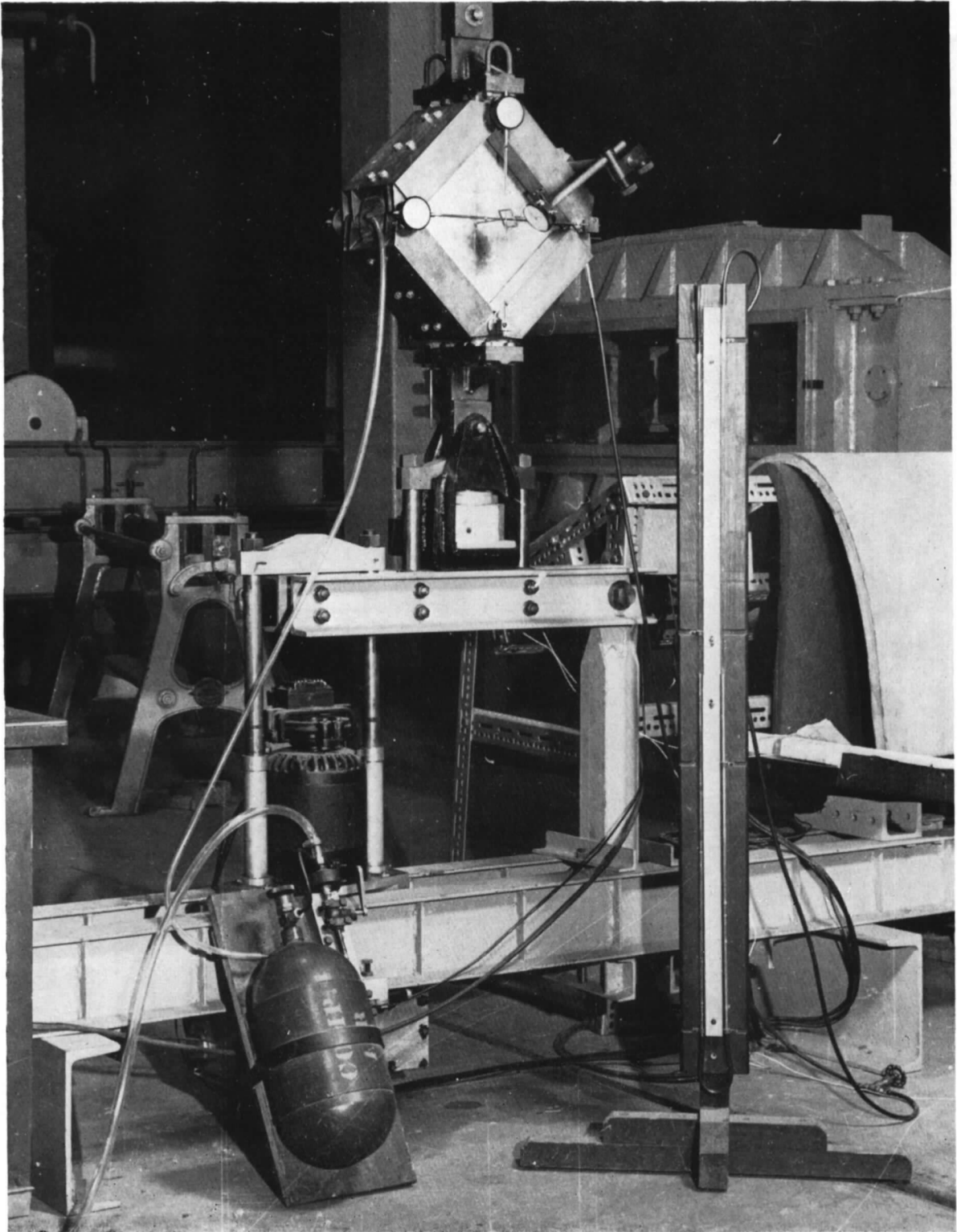
FIG. 6. Test rig for shear and pressure loading.

18
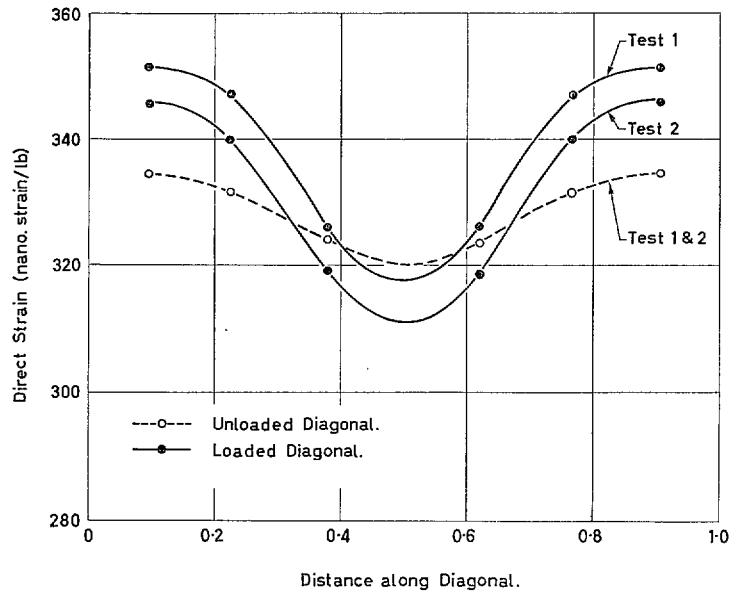
FIG. 7.   Strain distributions along panel diagonals.
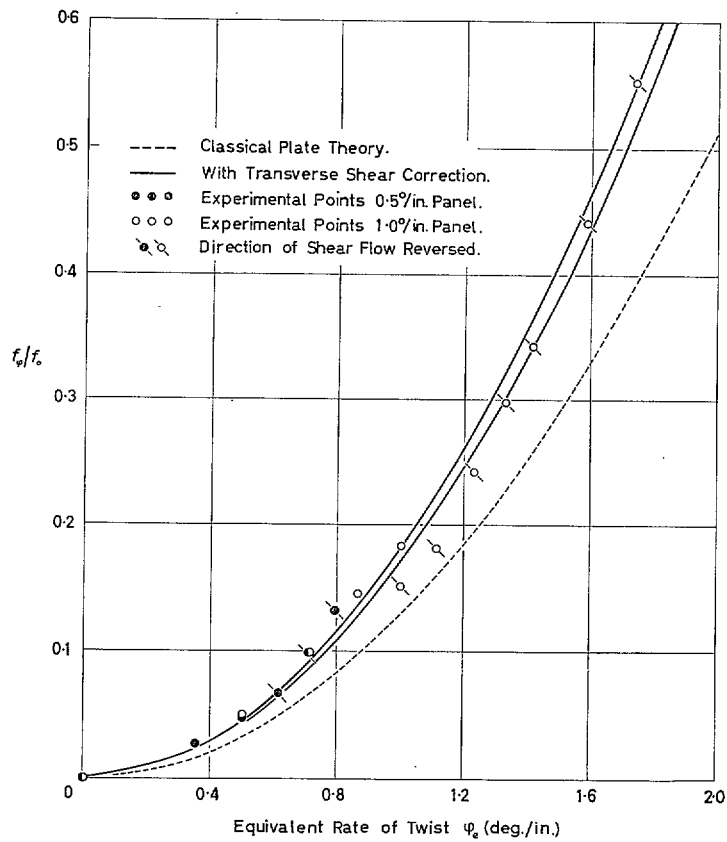
FIG. 8.   Increase of shear flexibility due to bending of twisted panels.

19

C
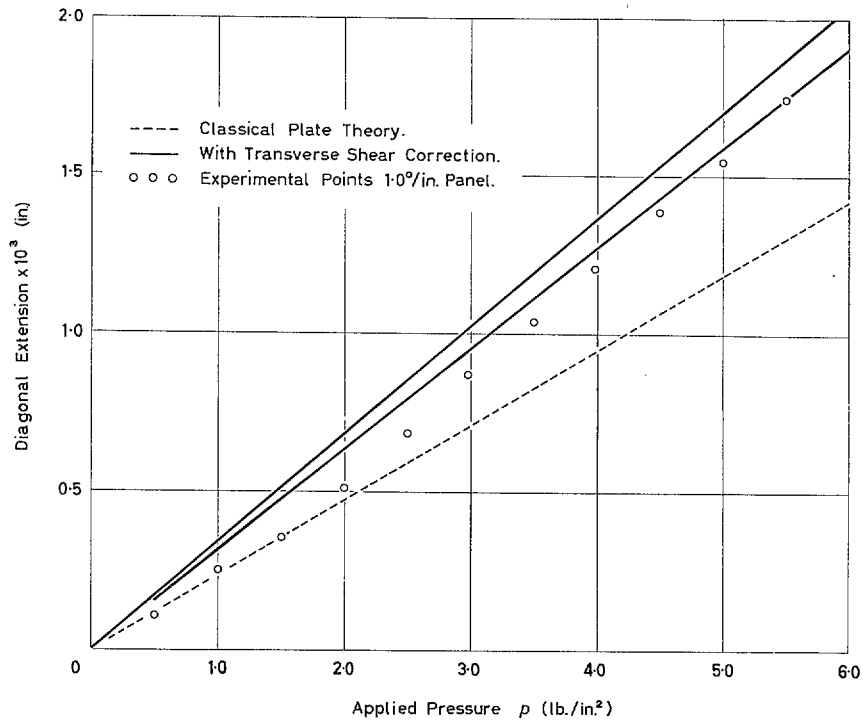
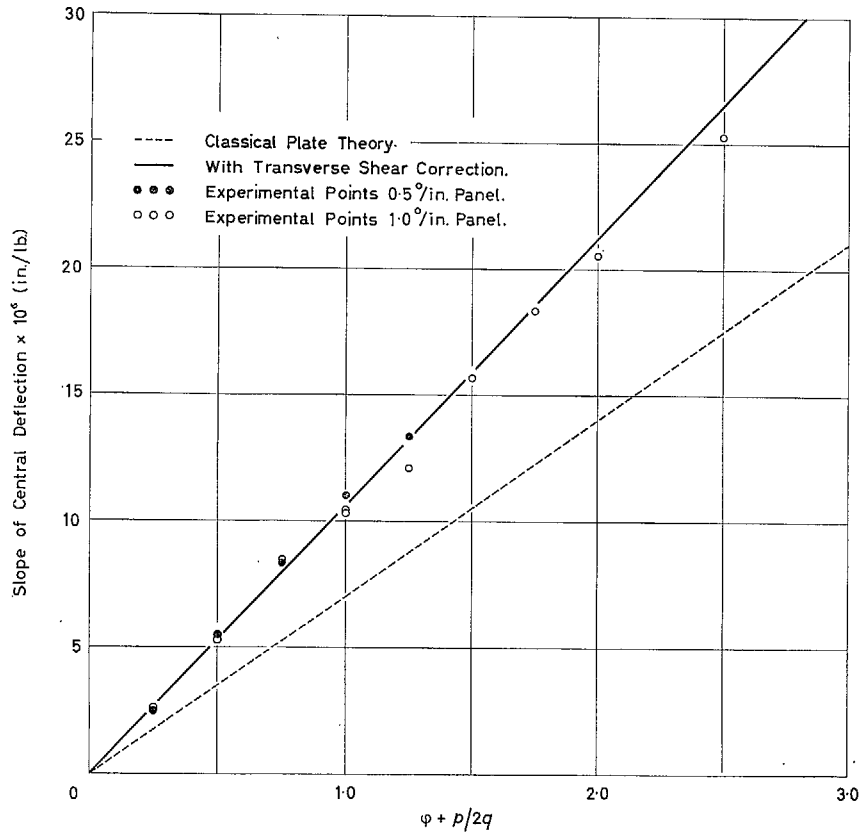FIG. 9. Shear strain of twisted panel due to normal pressure.

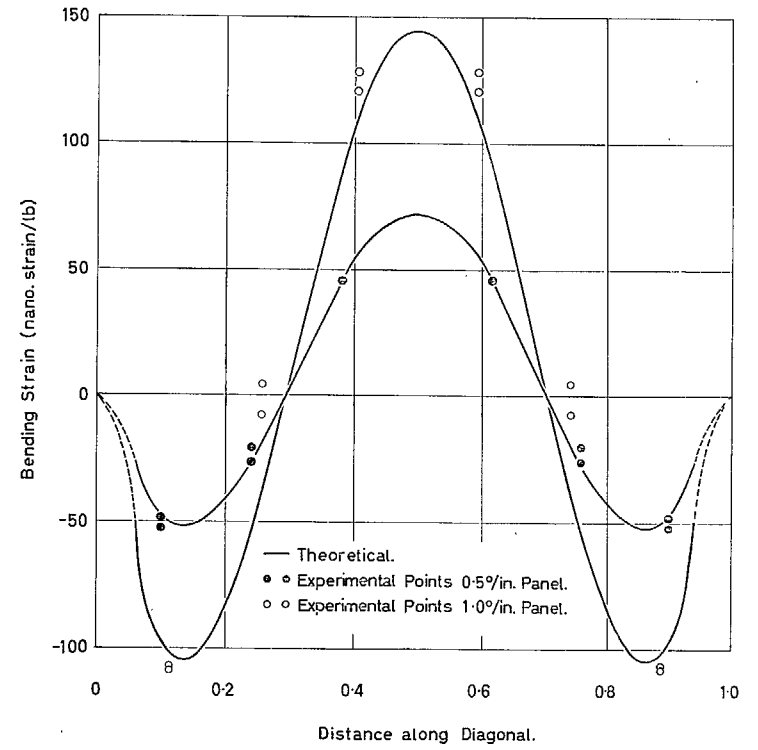FIG. 10.   Central deflections of twisted panel due to shear and pressure.

FIG. 11.   Bending-strain distribution along diagonal.

Publications of the
Aeronautical Research Council

ANNUAL TECHNICAL REPORTS OF THE AERONAUTICAL RESEARCH COUNCIL (BOUND VOLUMES)

1942 Vol. I. Aero and Hydrodynamics, Aerofoils, Airscrews, Engines. 75s. (post 2s. 9d.)
Vol. II. Noise, Parachutes, Stability and Control, Structures, Vibration, Wind Tunnels. 47s. 6d. (post 2s. 3d.)

1943 Vol. I. Aerodynamics, Aerofoils, Airscrews. 80s. (post 2s. 6d.)
Vol. II. Engines, Flutter, Materials, Parachutes, Performance, Stability and Control, Structures.
90s. (post 2s. 9d.)

1944 Vol. I. Aero and Hydrodynamics, Aerofoils, Aircraft, Airscrews, Controls. 84s. (post 3s.)
Vol. II. Flutter and Vibration, Materials, Miscellaneous, Navigation, Parachutes, Performance, Plates and Panels, Stability, Structures, Test Equipment, Wind Tunnels. 84s. (post 3s.)

1945 Vol. I. Aero and Hydrodynamics, Aerofoils. 130s. (post 3s. 6d.)
Vol. II. Aircraft, Airscrews, Controls. 130s. (post 3s. 6d.)
Vol. III. Flutter and Vibration, Instruments, Miscellaneous, Parachutes, Plates and Panels, Propulsion.
130s. (post 3s. 3d.)
Vol. IV. Stability, Structures, Wind Tunnels, Wind Tunnel Technique. 130s. (post 3s. 3d.)

1946 Vol. I. Accidents, Aerodynamics, Aerofoils and Hydrofoils. 168s. (post 3s. 9d.)
Vol. II. Airscrews, Cabin Cooling, Chemical Hazards, Controls, Flames, Flutter, Helicopters, Instruments and Instrumentation, Interference, Jets, Miscellaneous, Parachutes. 168s. (post 3s. 3d.)
Vol. III. Performance, Propulsion, Seaplanes, Stability, Structures, Wind Tunnels. 168s. (post 3s. 6d.)

1947 Vol. I. Aerodynamics, Aerofoils, Aircraft. 168s. (post 3s. 9d.)
Vol. II. Airscrews and Rotors, Controls, Flutter, Materials, Miscellaneous, Parachutes, Propulsion, Seaplanes, Stability, Structures, Take-off and Landing. 168s. (post 3s. 9d.)

1948 Vol. I. Aerodynamics, Aerofoils, Aircraft, Airscrews, Controls, Flutter and Vibration, Helicopters, Instruments, Propulsion, Seaplane, Stability, Structures, Wind Tunnels. 130s. (post 3s. 3d.)
Vol. II. Aerodynamics, Aerofoils, Aircraft, Airscrews, Controls, Flutter and Vibration, Helicopters, Instruments, Propulsion, Seaplane, Stability, Structures, Wind Tunnels. 110s. (post 3s. 3d.)

Special Volumes

Vol. I. Aero and Hydrodynamics, Aerofoils, Controls, Flutter, Kites, Parachutes, Performance, Propulsion, Stability. 126s. (post 3s.)
Vol. II. Aero and Hydrodynamics, Aerofoils, Airscrews, Controls, Flutter, Materials, Miscellaneous, Parachutes, Propulsion, Stability, Structures. 147s. (post 3s.)
Vol. III. Aero and Hydrodynamics, Aerofoils, Airscrews, Controls, Flutter, Kites, Miscellaneous, Parachutes, Propulsion, Seaplanes, Stability, Structures, Test Equipment. 189s. (post 3s. 9d.)

Reviews of the Aeronautical Research Council

1939-48 3s. (post 6d.)   1949-54 5s. (post 5d.)

Index to all Reports and Memoranda published in the Annual Technical Reports

1909-1947   R. & M. 2600 (out of print)

Indexes to the Reports and Memoranda of the Aeronautical Research Council

Between Nos. 2351-2449   R. & M. No. 2450   2s. (post 3d.)
Between Nos. 2451-2549   R. & M. No. 2550   2s. 6d. (post 3d.)
Between Nos. 2551-2649   R. & M. No. 2650   2s. 6d. (post 3d.)
Between Nos. 2651-2749   R. & M. No. 2750   2s. 6d. (post 3d.)
Between Nos. 2751-2849   R. & M. No. 2850   2s. 6d. (post 3d.)
Between Nos. 2851-2949   R. & M. No. 2950   3s. (post 3d.)
Between Nos. 2951-3049   R. & M. No. 3050   3s. 6d. (post 3d.)
Between Nos. 3051-3149   R. & M. No. 3150   3s. 6d. (post 3d.)

HER MAJESTY'S STATIONERY OFFICE

from the addresses overleaf